Journal of Geoscience and Environment Protection, 2025, 13(7), 99-110
https://www.scirp.org/journal/gep
ISSN Online: 2327-4344
ISSN Print: 2327-4336

Research on the Application of Transient Electromagnetic Method in Menkeqing Coal Mine

Fei Cao

College of Earth Science and Engineering, Xi'an University of Petroleum, Xi'an, China
Email: 969857548@qq.com

How to cite this paper: Cao, F. (2025). Research on the Application of Transient Electromagnetic Method in Menkeqing Coal Mine. *Journal of Geoscience and Environment Protection, 13*, 99-110.
https://doi.org/10.4236/gep.2025.137006

Received: May 25, 2025
Accepted: July 13, 2025
Published: July 16, 2025

Abstract

Coal mine water damage is a major hidden danger of mine safety production, threatening mine safety. In order to effectively prevent water damage, Menkeqing Coal Mine has carried out the research of electric method exploration, using transient electromagnetic method to detect the water-rich condition of strata. By analyzing the resistivity data and combining it with supplementary exploration, four major waterlogged areas in the mine were circled, and their spatial distribution and geological characteristics were clarified. The study shows that these methods are highly sensitive and accurate in identifying the water-rich layers, providing a reliable basis for the prevention and control of water hazards in coal mines, and helping to improve the level of mine safety and production.

Keywords

Transient Electromagnetic Method, Apparent Resistivity, Aquifer, Anomalous Zone

1. Introduction

Transient electromagnetic method detection technology has a 70-year application history in China (Wei et al., 2023), in the past 20 years, the transient electromagnetic detection technology has been constantly updated, and the alternating current method, including the transient electromagnetic method, the controllable-source audio geomagnetic method, and the mixed-source electromagnetic method, etc. have been rapidly developed (Fu, Kang, & Qiu, 2019). With its advantages of sensitive response to low resistance anomalies, strong directionality, small volume effect, high lateral resolution, high efficiency and low cost, the mine

transient electromagnetic method has achieved good application results in detecting hidden water-bearing (conductive) structures, water-filled boreholes, and water accumulation in the air-mining zone (Cui, 2019; Dong, Meng, & Zhao, 2023).

In this study, the mine transient electromagnetic method was used to carry out a detailed investigation of the water-bearing situation on the roof of the 11-3108 working face of the 3-1 coal seam in the Menkeqing coal mine, based on the theoretical basis of the transient electromagnetic method, the data processing and analysis of the apparent resistivity of the rock strata of the roof of the coal seam at the exploration working face was carried out, and on the basis of the existing technology, through the joint imaging of the iso-planar map of apparent resistivity of the roof of the coal seam in different layers, so as to achieve the comprehensive analysis of the horizontal and vertical. Thus, geological inference and interpretation can be carried out, so as to achieve the purpose of detecting the distribution of the coal seam and the upper aquifer, and to provide a reliable basis for the safe mining of the exploration face.

2. Study Area and Geological Background

2.1. Overview of the Study Area

Menkeqing Coal Mine is a supporting mine for the methanol to olefin and downstream polyolefin project (3.6 million tonnes/year) of Zhongtian Hetron Energy Co., Ltd. with a production scale of 12 million tonnes/a. The mine is located in the territory of Wuxian Banner and Yijinholo Banner of Ordos City, Inner Mongolia Autonomous Region, and administratively falls under the jurisdiction of Tuk Town of Wuxian Banner. The mine is located in the north-eastern part of Wutian Banner and the south-eastern part of Yijinholo Banner. As shown in **Figure 1**, the relative position of 11-3108 working face is southeast of the industrial square of the mine, mainly mining 3-1 coal, the thickness of the coal seam is 3.85-5.93, average 4.67 m. The east side of the working face is the big alley of the south wing of the 3-1 coal, the north side of the neighbouring 11-3106 working face (being mined back), the west side of the 11-3102 working face, the south side of the unmined area in the mine field.

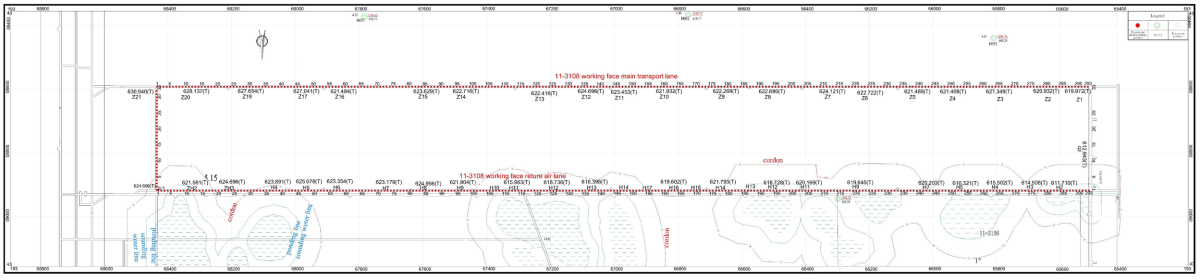

Figure 1. Schematic diagram of exploration scope.

2.2. Geological Overview

The direct water filling source of 3-1 coal roof is the sandstone fissure aquifer of

Jurassic Yan'an Formation and Zhiluo Formation within the scope of the development of the water-conducting fissure zone of the roof, while the indirect water filling source is the loose aquifer of the Cenozoic boundary, the porous submerged and pressurized water aquifer of the Shidan Group (K_1zh) of the Lower Cretaceous and the fissured and pressurized water aquifer of the Anding Formation of the Jurassic.

2.3. Geophysical Table Characteristics

11-3108 working face top plate stratum deposition is relatively smooth, 3-1 coal top plate exists Yan'an Group and Zhiluo Group sandstone aquifer, the strata itself fissure development will lead to aquifer local water-rich enhancement, and at the same time the north side of the working face 11-3106 is a mining area, the fissures are more developed after coal mining, also will lead to the local strata water-rich enhancement. The existence of physical changes provides good geophysical conditions for the effective application of mine transient electromagnetic (EM) with electrical differences as the detection premise.

3. Data Processing and Result Analysis

3.1. Transient Electromagnetic Principle

As a time-domain electromagnetic induction detection technology, the transient electromagnetic method is based on the following principle: firstly, a current pulse square wave is applied to the transmission loop, and when the leading edge of the square wave subsides, a primary magnetic field will be induced in the normal direction of the loop. This magnetic field excites the eddy current in the formation, and the strength of the vortex is closely related to the conductivity of the formation (Goldman, 1983). As the primary magnetic field decays, the eddy currents do not disappear immediately, but weaken in a gradual manner, resulting in a secondary magnetic field that decreases over time. This secondary magnetic field is extended to the receive loop and recorded. By analyzing the secondary induced electromotive force V under different time delays, the attenuation curves of the secondary magnetic field can be obtained, and the characteristics of the curves reveal the characteristics of the electrical distribution of the formation. If there is no high-efficiency conductor, the attenuation process is faster; however, the presence of a high-efficiency conductor delays the attenuation of the primary field, resulting in a significantly longer observed attenuation time, which in turn locates the position of the conductor see (see **Figure 2**).

The propagation mode of transient electromagnetic fields in the underground is analogous to the diffusion of "smoke rings", in which electromagnetic energy propagates directly in conductive formations and gradually dissipates. Affected by the skin-like effect, the high-frequency components are mainly confined to the vicinity of the surface, and the influence range is limited. In contrast, the low-frequency component is able to penetrate deeper formations, and its range of influence gradually expands with depth (see **Figure 3**).

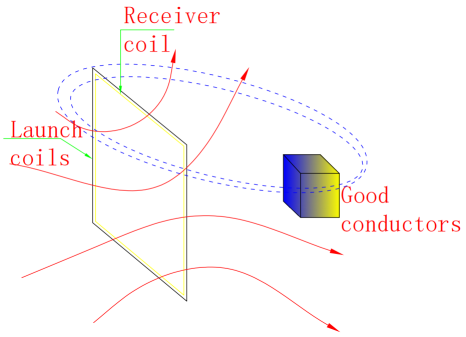

Figure 2. Schematic diagram of Transient electromagnetic induction of a good conductor.

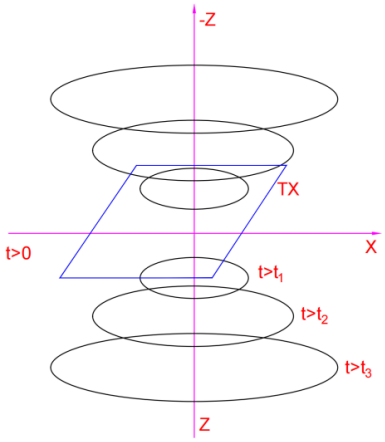

Figure 3. Full-space electromagnetic field "smoke ring effect".

3.2. Generalization of the Processing Method

The transient electromagnetic method is a method of detecting underground electrical structures by electromagnetic induction, using an ungrounded return line or a magnetic dipole to emit a primary field, and recording the secondary field signal generated by induction when the primary field disappears. The method is very sensitive to low-resistance bodies (e.g. waterlogged areas) and has the advantages of high resolution and small volume effects. By analyzing the temporal and spatial distribution of the secondary field signals, the electrical characteristics and geometric structure of the underground target can be inferred, which is particularly suitable for the detection of waterlogging in coal mining hollow areas. Data processing includes preprocessing, filtering, electromagnetic interference correction and inversion calculation.

Figure 4 shows the data processing flow, the data processing includes three links, data pre-processing; inversion of the data by establishing a model; and plotting the resistivity cross-section. Before processing the data collected in the field, the first point by point collation or pre-processing, that is, checking the quality of the data, eliminating unqualified data, and its cataloguing, organized into the order and format required by the special data processing software, and then filtering

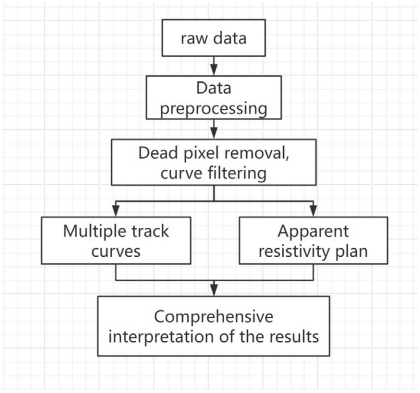

Figure 4. Data processing process.

of the data (as shown in **Figure 5** and **Figure 6**), in order to filter out or suppress the interference signal, to restore the change rule of the signal should be, highlighting the geological information, and then use the special software to convert to get the apparent resistivity and depth of visual and so on. parameters; on this basis, combined with relevant measurements, geological and drilling data to do further inferential processing; finally, the data obtained in the form of cross-section, slice contour plotted into a map, transient electromagnetic observation data is the transient induced voltage of each time window (channel) of each point, which needs to be converted into apparent resistivity, apparent depth, and other parameters, in order to carry out the next step in the interpretation of the data.

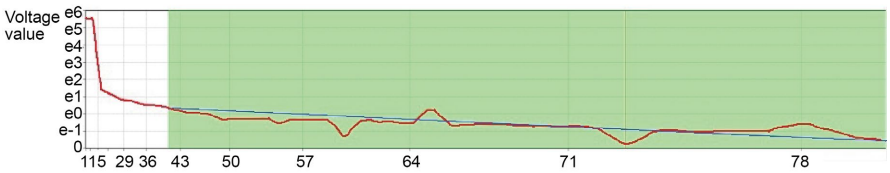

Figure 5. Induced voltage curve before filtering.

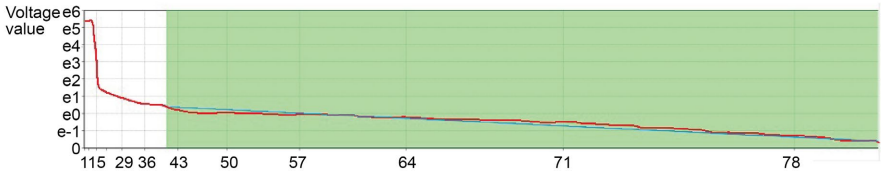

Figure 6. Induced voltage curve after filtering.

3.3. Determination of the Location of Aquifers

3108 working face has sandstone aquifer on the top of coal seam of Yan'an Formation of Middle Jurassic System at +20 m above the top plate, sandstone fissure aquifer of Yan'an Formation of Middle Jurassic System at +60 m above the top plate, and sandstone fissure aquifer of Zhiluo Formation of Middle Jurassic System at 100m above the top plate. Accordingly, the resistivity values of three different elevation sections near +20 m, +60 m and +100 m on the top plate of the

three coal seams were extracted for slicing and analysis, and the corresponding maps were drawn.

3.4. Determination of Thresholds

In a new coal mine application, when circling the water-rich anomalous area without comparative information, the measured apparent resistivity data are generally divided into five levels, which is $<\overline{\delta}-\delta_n$, $\overline{\delta}-\delta_n \sim \overline{\delta}-\delta_n/3$, $\overline{\delta}-\delta_n/3 \sim \overline{\delta}+\delta_n/3$, $\overline{\delta}+\delta_n/3 \sim \overline{\delta}+\delta_n$, $<\overline{\delta}+\delta_n$, and $\overline{\delta}-\delta_n/3$ can be set as the anomaly threshold. in the formula, $\overline{\delta}$ is the arithmetic mean value of the parameter and the δ_n is standard deviation value of the parameter. For values less than $\delta<\overline{\delta}-\delta_n/3$ can be set as the relative water-rich zone of each aquifer. The data processing and analysis of this time makes comprehensive use of electrical parameters combined with mathematical statistics to determine the basis for anomaly division and threshold value, and at the same time combines with the hydrogeological data in the exploration area and the actual situation of mining, and finally divides the water-rich zone of the aquifer.

The threshold value is determined with reference to the data from the nearby drill holes in the exploration area, and the mathematical and statistical method is combined with the change of resistivity in the plane and the hydrogeological situation. The final determination of the threshold value of low resistivity zone is shown in Table 1.

Table 1. Floor plan resistivity statistics.

Resistivity / stratum	maximum value (Ω·m)	minimum value (Ω·m)	average value (Ω·m)	standard deviation	Thresholds (Ω·m)
20 m above the roof of the coal seam	185.5	20.2	54.6	31.2	44.2
60 m above the roof of the coal seam	175.3	17.5	52.1	29.8	42.1
100 m above the roof of the coal seam	172.8	15.3	50.6	27.3	41.5

3.5. Plan View Analysis

(1) Analysis of apparent resistivity plan view near 20m on the top plate of 3108 working face

Figure 7 shows the 20m apparent resistivity plan view on the top plate of the 3108 working face, with a total of 4 relatively water-rich anomalies circled.

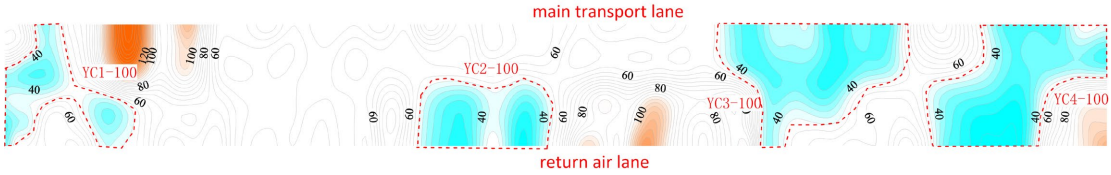

Figure 7. Plan view of 20 m apparent resistivity on the top plate of 11-3108 working face.

YC1-20 anomaly area is close to the side of the main transport lane, 100~160 m away from the starting point of the measurement line of the return air lane, 140~200 m within the working face (the return air lane points to the main transport lane), the anomalies are distributed in the form of a slice, the anomaly is small in scope, and the amplitude is weak. It is assumed that the degree of development of roof plate fissure in the anomaly area is weak, and it is suspected that there is a small amount of fissure water with weak water-rich nature.

The centre of YC2-20 anomaly area is close to the side of the return-air lane, and the anomalies are scattered in the range of 90~150 m from the starting point of the measurement line of the return-air lane (the return-air lane is pointing to the main transport lane), the anomalies have a relatively small scope and a weak amplitude. It is assumed that the degree of development of roof plate fissure in the anomaly area is weak, and it is suspected that there is a small amount of fissure water with weak water-rich nature.

The centre of YC3-20 anomaly area is close to the side of the return-air lane, and in the range of 0~250 m from the starting point of the measurement line of the return-air lane (the return-air lane points to the main transport lane), the anomalies are distributed in a piecemeal manner, with a larger scope and higher amplitude. It is assumed that the anomaly is caused by the relative water enrichment of the sandstone layer of the roof plate, and the water enrichment is strong.

YC4-20 anomaly centre is close to the side of the return lane, in the range of 2620~2780 m from the starting point of the measurement line of the return lane, and 0~240 m within the working face (the return lane is pointing to the main transport lane), the anomalies are distributed in a piecemeal form, with a medium range of anomalies and a general amplitude. It is assumed that the anomaly is caused by the relative water enrichment of the sandstone layer of the roof plate, and the water enrichment is general.

(2) Analysis of apparent resistivity map near 60m on the top plate of 3108 working face

Figure 8 shows the 60m apparent resistivity plan view on the top plate of the 3108 working face, with a total of 4 relatively water-rich anomalies circled.

YC1-60 anomaly area is close to the middle of the working face, 60~290 m away from the starting point of the measurement line of the return air lane, 60~240 m within the working face (the return air lane points to the main transport lane), the anomalies are distributed in scattered pieces, with a smaller anomaly range and a stronger amplitude. It is assumed that the anomaly is the development of roof plate fissure, and a small amount of fissure water is suspected to exist.

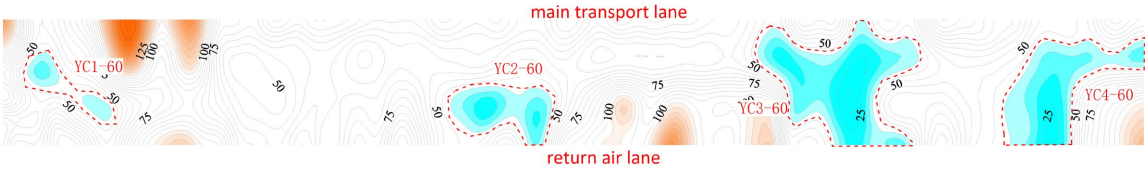

Figure 8. Plan view of 60m apparent resistivity on the top plate of 11-3108 working face.

The centre of YC2-60 anomaly area is close to the side of the main transport lane, and the anomalies are scattered and distributed in the range of 0~150m within the working face from the starting point of the measurement line of the return-air lane (the return-air lane is pointing to the main transport lane), the anomalies are relatively small in scope and the amplitude is strong. It is assumed that the anomaly is the development of roof plate fissure and suspected fissure water enrichment.

YC3-60 anomaly centre is close to the side of the return air lane, and in the range of 0~320m from the starting point of the measurement line of the return air lane to the main transport lane, the anomaly is distributed in the form of a slice, with a large anomaly range and a strong amplitude. It is assumed that the anomaly is caused by the relative water enrichment of the sandstone layer of the roof plate, and the water enrichment is strong.

The centre of YC4-60 anomaly area is close to the side of the return-air lane, and the anomaly is piecewise distributed in the range of 0~260m (the return-air lane is pointing to the main transport lane) from the starting point of the measurement line of the return-air lane at a distance of 2560~2919m, and the anomaly has a large range and strong amplitude. It is assumed that the anomaly is caused by the relative water enrichment of the sandstone layer of the roof plate, and the water enrichment is strong.

(3) Analysis of apparent resistivity map near 100m on the top plate of 3108 working face

Figure 9 shows the 100m apparent resistivity plan view on the top plate of the 3108 working face, with a total of 4 relatively water-rich anomalies circled.

YC1-100 anomaly area is close to the side of the main transport lane, in the range of 0~330m from the starting point of the measurement line of the return air lane, and 0~320m in the working face (the return air lane points to the main transport lane), the anomalies are distributed in scattered pieces, with a large range of anomalies and a medium amplitude. It is assumed that the anomalous layer is developed by fissure and suspected to be enriched by fissure water.

The centre of YC2-100 anomaly area is close to the side of the main transport lane, and the anomalies are scattered and distributed in the range of 0~160m in the working face from the starting point of the measurement line of the return-air lane (the return-air lane is pointing to the main transport lane), the anomalies have a medium range and a strong amplitude. It is assumed that the anomaly is caused by the relative water enrichment of the sandstone layer of the roof plate.

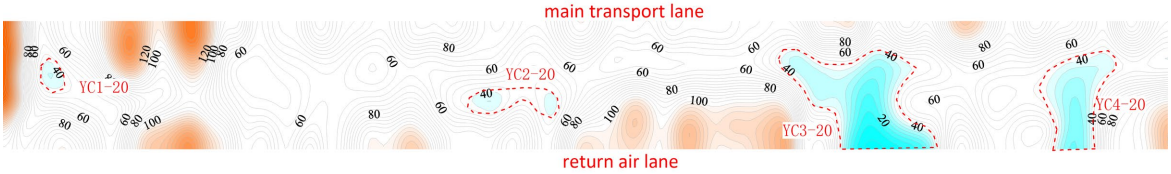

Figure 9. Plan view of 100m apparent resistivity on the top plate of 11-3108 working face.

YC3-100 anomaly centre is close to the side of the return wind lane, in the range of 0~320 m from the starting point of the measurement line of the return wind lane to the working face (the return wind lane is pointing to the main transport lane), the anomaly is distributed in the form of a slice, with a large anomaly range and a strong amplitude. It is assumed that the anomaly is caused by the relative water enrichment of the sandstone layer of the roof plate, and the water enrichment is strong.

The centre of YC4-100 anomaly area is close to the side of the return-air lane, and in the range of 0~320 m (the return-air lane is pointing to the main transport lane), the anomalies are distributed in a piecemeal manner, with a large anomaly range and a strong amplitude from the starting point of the measurement line of the return-air lane, which ranges from 2450~2919 m. It is assumed that the anomaly is caused by the relative water enrichment of the sandstone layer of the roof plate, and the water enrichment is strong.

3.6. Geological Inference

Figure 10 shows a plan view of the apparent resistivity of the different elevation sections above the top slab of the 3108 working face. From the figure, it can be seen that within 110 m above the top plate of No.3 coal seam in 3108 working face, there are mainly four low resistivity anomalies developed.

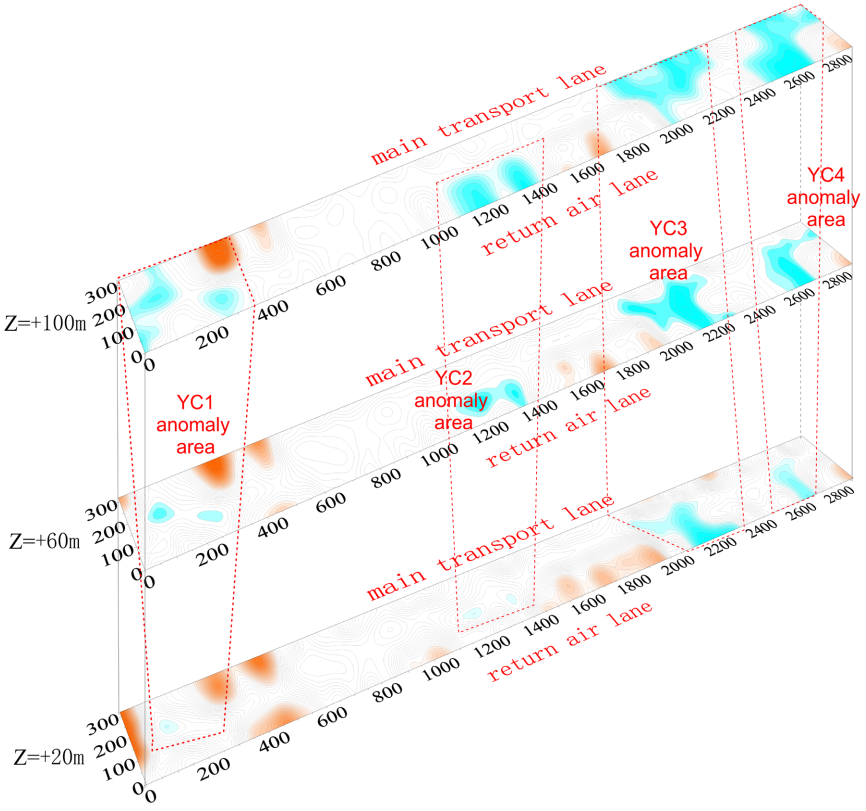

Figure 10. Plan view of apparent resistivity of different elevation sections of 3108 working face.

The range and amplitude of anomalies in anomaly area YC1 gradually increase with the increase of height, and the amplitude gradually strengthens. It can be seen from the vertical development that the anomalies of the +20 m layer section are weakly water-rich, and the water-richness of the +60 m and +100 m layer sections is a little stronger, but the anomalies are generally more dispersed, so it is assumed that the fissures of the +60 m and +100 m layer sections are weakly developed, and the degree of fissure development of the +20 m layer section and the upper sandstone layer is assumed to be weak or even undeveloped. The degree of fissure development in the upper sandstone layer of the +20 m layer is weak or even undeveloped.

The anomaly range and amplitude of anomaly area YC2 gradually become larger with the increase of height, and the amplitude gradually strengthens. From the vertical development, it can be seen that the anomaly range of +20 m layer section is small, and the anomaly ranges of +60 m and +100 m layers are much larger than that of +20 m layer section, so it is assumed that the water-richness of sandstone in the +20 m layer section of this area is weak, and that the water-richness of the +60 m and +100 m layer section is stronger, and the water-richness of the suspected +20 m layer section is weak, and that the water-richness of the +20m layer section is weak. It is suspected that the +20 m layer has a low or even no degree of fracture development with the upper sandstone layer.

The anomaly range and amplitude of YC3 anomaly area gradually become larger with the increase of height, and the amplitude gradually strengthens, and it can be seen from the vertical development situation that the water-rich nature shows the change rule of "from low to high" from the bottom to the top. Combined with the geological data, it is assumed that the upper part of the coal seam roof plate is cracked, and it is suspected that the sandstone aquifer of Yan'an Formation and the sandstone aquifer of Zhi Luo Formation are connected, which makes the sandstone layer relatively water-rich.

The anomaly range and anomaly amplitude of YC4 anomaly area gradually become larger with the increase of height, and the amplitude gradually strengthens, and it can be seen from the vertical development situation that the water-rich nature shows the change rule of "from low to high" from the bottom to the top. The anomalous range and amplitude of +20 m layer section are relatively small, and the anomalous range and amplitude of +60 m and +100 m layer section increase abruptly, so it is assumed that the degree of fissure development in the +20 m layer section is weak, and the degree of fissure development in the +60 m and +100 m layer section is high, which results in the enhancement of water-richness of the aquifer.

To sum up: 3108 working face top plate within 100 m 3 slices results, 3108 working face top plate +20 m for the Jurassic middle Yan'an group coal seam top sandstone aquifer water-rich nature of weak ~ weak; top plate +60 m for the Jurassic middle Yan'an group sandstone fissure aquifer water-rich nature of weak; top plate 100 m for the Jurassic middle Zhi Luo group sandstone fissure aquifer

water-rich nature of medium. According to the existing geological data: there is no 2-2 coal seam mining area above the top plate, and 11-3106 mining area on the north side, so there is a fissure zone developing at the top of the side close to the return airway. The water-richness of 0~100 m water-bearing layer on the top plate of the working face is "strong~weak" from the top to the bottom, and the connectivity between the top plate +20 m and +60~+100 m is poor, and there is a certain spatial similarity between the top plate +60 m and +100 m, and there is a slight development of fissure at the similar position of the stratum, which makes the water-richness of the water-bearing layer relatively good.

4. Conclusion

In this study, the transient electromagnetic method was applied to detect and analyze the water-rich condition of the upper aquifer in the 11-3108 working face of Menkeqing Coal Mine, and the results of the detection revealed a number of low-resistance anomalous zones, and these anomalous zones accurately reflect the location and geological characteristics of the main water accumulation zones of the upper aquifer, which provide accurate target zones for the roof dredging and draining project in the later stage of the working face. The study shows that the transient electromagnetic method can effectively detect the water-rich condition of the formation under complex geological conditions with high sensitivity and accuracy. The research results provide important technical support for the prevention and control of water damage in Menkeqing Coal Mine, and provide a scientific basis for the prevention and control of water damage in similar mines. In the future, further combining with other geophysical detection means, it is expected to improve the precision and efficiency of waterlogging area detection, so as to better protect the safe production of coal mines.

Conflicts of Interest

The author declares no conflicts of interest regarding the publication of this paper.

References

Cui, X. (2019). A Study on Detection of Goaf Water of Tianli-Tianxin Coal Mine Based on Transient Electromagnetic Method. *Journal of Physics: Conference Series, 1176,* 062055. https://doi.org/10.1088/1742-6596/1176/6/062055

Dong, H. Y., Meng, Z. Q., & Zhao, Z. H. (2023). Application of Transient Electromagnetic Method in Goaf Detection. *Journal of Research in Science and Engineering, 5,* 18-22. https://doi.org/10.53469/JRSE.2023.05(05).04

Fu, Z. Y., Kang, J., Qiu, D. W. (2021). In Situ Measurement of Water Accumulation in Overlying Goaf of Coal Mine-A Transient Electromagnetic-Based Study. *Arabian Journal of Geosciences, 14,* Article No. 406. https://doi.org/10.1007/s12517-021-06771-7

Goldman, M. M. (1983). The Integral-Finite-Difference Method for Calculating Transient Electromagnetic Fields in a Horizontally Stratified Medium. *Geophysical Prospecting, 31,* 664-686. https://doi.org/10.1111/j.1365-2478.1983.tb01078.x

Wei, Z., Dong, J., Zhao, M., Xie, F., Li, Y., & Feng, L. (2023). Transient Electromagnetic

Detection and Numerical Simulation Analysis of the Deformation Characteristics of an Old Goaf in an Alpine Coal Mine Area. *Frontiers in Earth Science, 11,* 1-15. https://doi.org/10.3389/feart.2023.1220142